Beni-Suef University Journal of Basic and Applied Sciences

RESEARCH

Open Access

Analytical solution of thermal effect on unsteady visco-elastic dusty fluid between two parallel plates in the presence of different pressure gradients

Mohamed Elshabrawy[1,2*], Osama Khaled[3], Wael Abbas[4], Salah-Eldeen Beshir[1] and Mostafa Abdeen[5]

Abstract

Background Thermal diffusion of dusty fluids has valuable interference in various fields, including waste-water treatment, oil transportation, and power plant pipes. Dusty fluids are used in lots of industrial fields as a result of their improved heat transfer and heat management capabilities. These industries range from renewable energy systems to aerobic plastic sheet extrusion, manufacturing, and rolling and reaching metal sheet cooling.

Results The work embodied in this paper presents the analytical solution performed to predict the effects of thermal diffusion on dusty, viscous, incompressible fluid flows between two porous, parallel vertical plates with a heat source or a heat sink. The mathematical equations are solved by the separation of variables and Laplace transform techniques. The influence of temperature is investigated for various values of Prandtl number and heat source or heat sink parameters. Also, the influences of various coefficients like the thermal diffusion coefficient, Schmidt number, Prandtl number, and heat source or heat sink coefficient on the concentration are observed. The fluid velocity distribution is graphically obtained. The solutions are discussed and exhibited graphically. The influences of the thermal diffusion parameter and chemical reaction parameter on fluid and dust particles' velocities are examined. A parametric study on the effect of time on temperature and concentration is made.

Conclusions The exact expressions for temperature, concentration, and velocity variation for fluid and dusty particles are obtained analytically. The temperature is inversely proportional to both the Prandtl number Pr and the heat source or heat sink parameter H_S. The concentration of the fluid is inversely proportional to the thermal diffusion parameter *Td* and the heat source or heat sink parameter H_S.

Keywords Dusty viscous, Incompressible fluid, Thermal diffusion, Concentration, Velocity profile, Pressure gradient

*Correspondence:
Mohamed Elshabrawy
mmshabrawy@nu.edu.eg
Full list of author information is available at the end of the article

1 Background

Thermal diffusion of dusty fluids has always been a point of interest to researchers as well as practitioners owing to its valuable interference in various fields, including wastewater treatment, oil transportation, and power plant pipes. Dusty fluids have paved their way through lots of industrial fields as a result of their improved heat transfer and heat management capabilities; these industries range from renewable energy systems to aerobic plastic sheet extrusion, manufacturing, and rolling metal sheet cooling. Nidhi et al. [1] have studied the unsteady magnetohydrodynamics (MHD) Walter's-B viscoelastic dust effect of vibration temperature on fluids passing through inclined porous plates with thermal radiation.

Farhad et al. [2] investigated the effects of a magnetic field paired with heat transfer on conductive, viscoelastic, incompressible, and dusty fluids moving between two non-conductive inflexible plates. Radhika [3] and [4] have studied the effect of heat transfer on dusty liquids with hybrid nanoparticles floating on the molten surface. Bilal et al. [5] discussed the Couette flow of dusty viscoelastic fluid in a rotating frame with heat transfer. Mallikarjuna et al. [6] investigated the effect of radiation and thermal diffusion on the MHD heat transfer flow of a dusty, viscous, incompressible conductive fluid between two parallel plates. Govindarajan et al. [7] studied the combined impacts of mass and heat transmission on a radiant MHD oscillating thin dusty fluid in a fully saturated permeable channel.

The study of chemical reactions and thermal diffusion has many applications, including liquid metal cooling of nuclear processes, sustained plasma confinement for controlled thermonuclear fusion, and electromagnetic metal casting. K. Suneeth et al. [8] have studied the effect of thermal radiation on the flow of MHD viscoelastic fluid through a porous movable plate with a primary chemical reaction. Debasish Dey [9] made a numerical model to study and analyze the dusty fluid flowing through a vertical surface with heat-generating and endothermic-type chemical reactions. Prasanthi et al. [10] have investigated the upshots of chemical reactions and radiations on MHD dusty flow over a sloping porous sheet immersed in a porous medium.

Furthermore, it is mentioned that other researchers studied the influence of pressure gradients on dusty fluid flow. Kanaka Lata Ojha et al. [11] have studied the influence of sinusoidal gradients of pressure upon two-dimensional unsteady viscoelastic hydromagnetic currents through channels lined by porous materials. Dash et al. [12] have studied the effect of a sinusoidal pressure gradient on viscoelastic hydromagnetic flow between two porous parallel plates. MHD's dusty fluid flow has witnessed heavy research and has grabbed researchers' attention for quite some time. Jadav Konch [13] has developed computer codes to study outcomes at the unsteady glide of a viscous dusty fluid beyond an exponentially increased vertical plate with viscous dissipation within the existence of a warmth supply and magnetic field. Bilal [14] has numerically discussed the influence of Hall currents on the unsteady rotating current of carbon nanotubes in a permeable Darcy–Forchheimer media with dust grains and nonlinear heat radiation. Dawar [15] has investigated the Hall effect in dual-phase radiative dusty nanofluid flow across a stretched sheet. Neetu Singh et al. [16]] have investigated the effect of inertia on dusty fluid in a permeable medium. Chitra et al. [17] have studied the flow of an unsteady dusty fluid across an impermeable media in a circular pipe under the influence of a magnetic field and a time-varying pressure gradient with slip conditions. Sudhir Kumar [18] has studied, using linearized theory, the influences of dust particles, rotation, couple stress, and magnetization on a thin film of couple stress magnetized fluid's thermal stability. Sasikala [19] focused on adding dust particles between two parallel plates passing through a permeable media in the existence of a magnetic field. He observed that the upper plate has a uniform suction force, while the bottom plate has a constant injection. Farhad Ali et al. [20] have discussed the fluctuating natural convection of heat-absorbing viscoelastic dust liquid in horizontal channels with the MHD infusion.

Analytical methods are often the preferred approach for solving partial differential equations (PDEs) [21] when it is possible to do so. This is because analytical solutions are often more accurate than numerical solutions, and they can be more easily generalized to other problems [4, 22]. Some of the most common analytical methods for solving PDEs include separation of variables [23], Fourier transforms [24], Laplace transforms, and Green's functions. Marwan Al-Raeei [24] derived the bulk modulus relationship for the Morse interaction, by using the Fourier transformation and the mean-spherical approximation.

The purpose of this investigation is to derive an analytical solution by using the separation of variables method to discuss the effect of heat on the unsteady, dusty viscoelastic fluid in the presence of different pressure gradients. The problem is formulated and analytically solved, and the relevant results are discussed in depth graphically to explore the influence of various fluid parameters.

2 Method

2.1 Governing equations

The problem considered is a flow of an incompressible viscous dusty fluid between two infinite plates separated by a

distance 2*h* without body force as illustrated in Fig. 1 based on the aforementioned assumptions

- The flow is unsteady, laminar, and subjected to pressure gradient varying over time the plate movement
- The flow passes through two parallel plates that are vertically heated and have a heat source or sink.
- In the beginning, the fluid and dust particle clouds will both be expected to be stationary.
- The dust particles are considered to be homogeneous in size with a spherical shape.
- The dust particle number density is assumed to be uniform.
- The flow in a porous medium.

The governing equations [25] are:

$$\frac{\partial u}{\partial t} = -\frac{1}{\rho}\frac{\partial P}{\partial x} + g\beta(T - T_0) + g\beta(C - C_0) + \gamma\left(1 - \lambda\frac{\partial}{\partial t}\right)\frac{\partial^2 u}{\partial y^2} + \frac{kN}{\gamma}(v - u) - \frac{\gamma}{k}u \tag{1}$$

$$\frac{\partial v}{\partial t} = \frac{k}{m}(u - v) \tag{2}$$

$$\frac{\partial T}{\partial t} = \frac{K_T}{\rho C_p}\frac{\partial^2 T}{\partial y^2} - \frac{Q_1}{\rho C_p}(T - T_0) \tag{3}$$

$$\frac{\partial C}{\partial t} = D\frac{\partial^2 C}{\partial y^2} - \alpha(C - C_0) + D_T\frac{\partial^2 T}{\partial y^2} \tag{4}$$

The initial and boundary condition are

$$\begin{aligned} &t = 0, u = v = 0, T = T_0, \mathrm{C} = \mathrm{C_o}, \quad -\mathrm{h} < \mathrm{y} < \mathrm{h} \\ &t > 0, u = v = 0, = To + (\mathrm{T_w} - \mathrm{T_o})\left(1 - \mathrm{e}^{-\mathrm{at}}\right), \text{and} \\ &C = \mathrm{Co} + (\mathrm{Cw} - \mathrm{Co})\left(1 - \mathrm{e}^{-\mathrm{at}}\right), \quad \mathrm{y} = \pm\mathrm{h} \end{aligned} \tag{5}$$

where u—fluid velocity (m/s), t—time (s), ρ—fluid density (kg/m^3), P—pressure of the fluid (N/m^2), x-axis of co-ordinates oriented along the flow direction. (m), g—gravity acceleration (m/s^2), β—coefficient of volumetric thermal expansion ($1/°C$), T—fluid temperature ($°C$), T_o—initial temperature ($°C$), C fluid concentration (kg/m^3), C_0—initial uniform concentration at T_0, γ—kinematic viscosity (Ns/m^2), λ—the diffusing particles' mean free path, y—normal to the plate coordinate axis (m), k—non-dimensional chemical reaction coefficient, N—the particle density number of the dust, v—dust particles velocity (m/s), m—mass of the dust particles (kg), $K_\mathrm{T}-$ the fluid's thermal conductivity coefficient (W m^{-1} K^{-1}) $C_{\mathrm{P}-}$ specific heat at constant pressure (J/kg K), Q_1—volumetric heat generation or absorption rate (W/m^2), D—rate of mass diffusion (m^2/s), α—chemical reaction coefficient, D_T—thermal diffusion coefficient (m^2/s). C_w—concentration at the wall, and T_w—temperature at the wall

Considering the following dimensionless quantities

$$\begin{aligned} P^* &= \frac{P}{\gamma\rho}, \quad y^* = \frac{y}{h}, x^* = \frac{x}{h} \\ u^* &= \frac{u}{h}, \quad v^* = \frac{v}{h}, t^* = \frac{\gamma t}{h^2} \\ a^* &= \frac{ah^2}{\gamma}, \quad T^* = \frac{T_0 - T}{T_0 - T_w}, C^* = \frac{C_0 - C}{C_0 - C_w} \end{aligned} \tag{6}$$

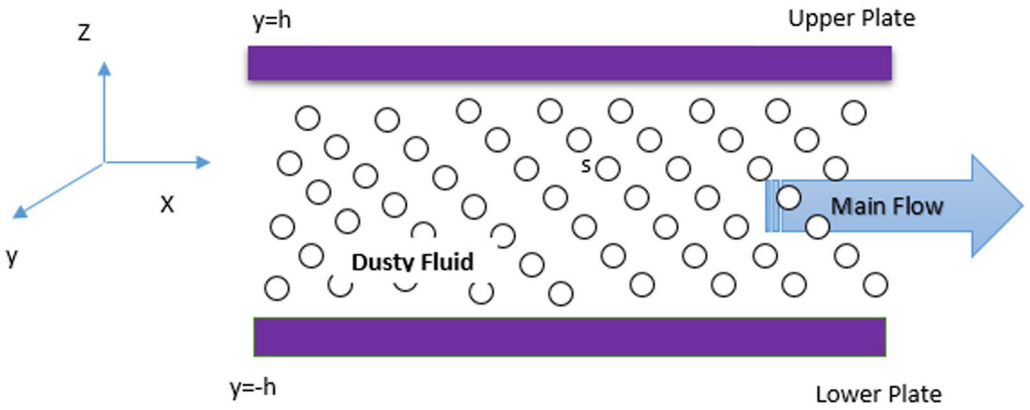

Fig. 1 Geometry of the flow

The governing equations are reduced to

$$\frac{\partial u}{\partial t} = -\frac{\partial P}{\partial x} + G_r T + G_m C + \gamma\left(1 - V_e\frac{\partial}{\partial t}\right)\frac{\partial^2 u}{\partial y^2} + \frac{1}{\tau}(v-u) - \frac{u}{M} \tag{7}$$

$$\frac{\partial v}{\partial t} = \frac{1}{r}(u-v) \tag{8}$$

$$\frac{\partial^2 T}{\partial y^2} - P_r\frac{\partial T}{\partial t} - H_s T = 0 \tag{9}$$

$$\frac{\partial^2 C}{\partial y^2} - S_c\frac{\partial C}{\partial t} - C_r S_c C + T_d\frac{\partial^2 T}{\partial y^2} = 0 \tag{10}$$

The initial and boundary conditions are given by

$$\begin{aligned} &t = 0, u = v = T = C = 0, -1 < \mathrm{y} < 1 \\ &t > 0, u = v = 0, T = \left(1 - e^{-at}\right) \text{ and } C = \left(1 - e^{-at}\right), y = \pm 1 \end{aligned} \tag{11}$$

where Grashof number (1/°K) $G_r = g\beta h\frac{T_w - T_0}{\gamma}$, modified Grashof number (1/°K) $G_m = g\beta h\frac{C_w - C_0}{\gamma}$, visco-elastic parameter $V_e = \frac{\gamma\lambda}{h^2}$, mass concentration of dust particle g/m^3 $l = \frac{\gamma m}{kh^2}$, Prandtl number $P_r = \mu\frac{C_P}{K_T}$, source or sink parameter for heat $H_s = \frac{Q_1}{K_T}h^2$, Schmidt number $S_c = \frac{\gamma}{D}$, dimensionless parameter of a chemical reaction $C_r = \frac{\alpha h^2}{\gamma}$, parameter of thermal diffusion $T_d = \frac{D_T}{D}\left(\frac{T_W - T_0}{C_W - C_0}\right)$, the fluid viscosity $\mu = \gamma\rho$, and chemical reaction parameter $M = \frac{K}{h^2}$

2.2 Analytical solution

Starting with the homogenous differential equation for temperature

$$\frac{\partial^2 T(y,t)}{\partial y^2} - P_r\frac{\partial T(y,t)}{\partial t} - H_s T(y,t) = 0 \tag{12}$$

it is subjected to non-homogenous boundary conditions

$$\begin{aligned} &t = 0, T = 0, y\epsilon(-1,1) \\ &t > 0, T = \left(1 - e^{-at}\right), y = \pm 1 \end{aligned} \tag{13}$$

To solve this differential equation by using the method of separation of variables, which is one of the most popular methods for solving partial differential equations, and assuming that the solution is separable, that is, the final solution can be formulated as a product of different functions, each of which is only dependent on a single independent variable [23]. We first transform the non-homogenous boundary conditions into homogeneous ones by assuming that

$$T(y,t) = \left(1 - e^{-at}\right)\frac{\cosh\left(m_1 y\right)}{\cosh\left(m_1\right)} + T^*(y,t) \tag{14}$$

Substituting Eq. 14 in Eq. 12 we get

$$\begin{aligned} \tfrac{\partial^2 T^*(y,t)}{\partial y^2} - P_r\tfrac{\partial T^*(y,t)}{\partial t} - H_s\ T^*(y,t) &= F(y,t) \\ \text{at } t = 0 \qquad T^* &= 0 \qquad y \in (-1,1) \\ \text{at } t > 0 \qquad T^* &= 0 \qquad y = \pm 1 \end{aligned} \tag{15}$$

where

$$\begin{aligned} F(y,t) &= \left(\gamma_3 + \gamma_2 e^{-at}\right)\frac{\cosh\left(m_1 y\right)}{\cosh\left(m_1\right)}, \\ \gamma_3 &= \left(H_s - m_1^2\right), \gamma_2 = (P_r a - \gamma_3) \end{aligned} \tag{16}$$

Equation 15 is a homogenous partial differential equation with homogenous boundary conditions that will be analyzed via the method of separation of variables. We can firstly solve the homogenous one

$$\frac{\partial^2 T^*(y,t)}{\partial y^2} - P_r\frac{\partial T^*(y,t)}{\partial t} - H_s T^*(y,t) = 0 \tag{17}$$

assume

$$T^*(y,t) = T^*(t)T^*(y) \tag{18}$$

by substituting Eq. 18 in Eq. 17 we get

$$T^*(t)T^{*\prime\prime}(y) - P_r T^{*'}(t)T^*(y) - H_s T^*(t) \quad T^*(y) = 0 \tag{19}$$

$$\therefore \frac{T^{*\prime\prime}(y)}{T^*(y)} - P_r\frac{T^{*\prime}(t)}{T^*(t)} - H_s = 0 \tag{20}$$

$$\therefore \frac{T^{*\prime\prime}(y)}{T^*(y)} = P_r\frac{T^{*\prime}(t)}{T^*(t)} + H_s = -\lambda^2 \tag{21}$$

$$\therefore T^{*\prime\prime}(y) + \lambda^2 T^*(y) = 0 \tag{22}$$

and

$$P_r\frac{T^{*\prime}(t)}{T^*(t)} + H_s = -\lambda^2 \tag{23}$$

$$\therefore P_r T^{*\prime}(y) + \left(H_s + \lambda^2\right) T^*(t) = 0 \tag{24}$$

The solution of Eq. 22 is

$$\begin{aligned} &T^*(y) = l_1 \cos(\lambda y) + l_2 \sin(\lambda y) \\ &\text{at } y = 1 \quad T^* = 0 \to 0 = l_1 \cos\lambda + l_2 \sin\lambda \\ &\text{at } y = -1 \quad T^* = 0 \to 0 = l_1 \cos\lambda - l_2 \sin\lambda \\ &\qquad \text{Then by addition, we get } 2l_1 \cos\lambda = 0 \\ &l_1 \neq 0 \quad \therefore \cos\lambda = 0 \to \quad \lambda = \frac{2n-1}{2}\pi, \quad n = 1, 2, 3, \ldots \\ &0 = l_1 \cos\lambda - l_2 \sin\lambda \\ &0 = C \cos\left(\frac{2n-1}{2}\pi\right) + l_2 \sin\left(\frac{2n-1}{2}\pi\right) \therefore l_2 = 0 \end{aligned} \tag{25}$$

$$\therefore T^*(y) = l_1 \cos\left(\frac{2n-1}{2}\pi\right) y \tag{26}$$

This function is the eigen function for solving the non-homogeneous partial differential equation

$$T^*(y,t) = \sum_{n=1}^{\infty} T_n^*(t) \cdot \cos\left(\frac{2n-1}{2}\pi\right) y \tag{27}$$

$$\frac{\partial^2 T^*(y,t)}{\partial y^2} - P_r \frac{\partial T^*(y,t)}{\partial t} - H_s T^*(y,t) = F(y,t) \tag{28}$$

$$F(y,t) = \sum_{n=1}^{\infty} F_n(t) \cdot \cos\left(\frac{2n-1}{2}\pi\right) y \tag{29}$$

$$\begin{aligned} &\frac{\partial^2 T^*(y,t)}{\partial y^2} - P_r \frac{\partial T^*(y,t)}{\partial t} - H_s T^*(y,t) \\ &= \sum_{n=1}^{\infty} F_n(t) \cdot \cos\left(\frac{2n-1}{2}\pi\right) y \\ &T^* = 0 \quad \text{at} \quad t = 0 \\ &T^* = 0 \quad \text{at} \quad y = \pm 1 \end{aligned} \tag{30}$$

Then the solution is

$$T^*(y,t) = \sum_{n=1}^{\infty} T_n^*(t) \cdot \cos\left(\frac{2n-1}{2}\pi\right) y \tag{31}$$

Substitute Eq. 31 in Eq. 30 we can get

$$\begin{aligned} &\sum_{n=1}^{\infty} -\left(\frac{2n-1}{2}\pi\right)^2 T_n^*(t) \cos\left(\frac{2n-1}{2}\pi\right) \\ &- \sum_{n=1}^{\infty} P_r \frac{dT_n^*(t)}{dt} \cos\left(\frac{2n-1}{2}\pi\right) y \\ &- H_s \sum_{n=1}^{\infty} T_n^*(t) \cos\left(\frac{2n-1}{2}\pi\right) y \\ &= \sum_{n=1}^{\infty} F_n(t) \cdot \cos\left(\frac{2n-1}{2}\pi\right) y \end{aligned} \tag{32}$$

where

$$F(y,t) = \sum_{n=1}^{\infty} F_n(t) \cos\left(\frac{2n-1}{2}\pi\right) y \tag{33}$$

By orthogonality

$$\begin{aligned} \int_{-1}^{1} F(y,t) \cos\left(\frac{2m-1}{2}\pi\right) y dy = \sum_{n=1} \int_{-1}^{1} F_n(t) \\ \left\{\cos\left(\frac{2n-1}{2}\pi\right) y\right\} \\ \left\{\cos\left(\frac{2m-1}{2}\pi\right) y\right\} dy \end{aligned} \tag{34}$$

For

$$\begin{aligned} m = n \quad &\int_{-1}^{1} \cos\left(\frac{2n-1}{2}\pi\right) y \cos\left(\frac{2m-1}{2}\pi\right) y dy = 1 \\ m \neq n \quad &\int_{-1}^{1} \cos\left(\frac{2n-1}{2}\pi\right) y \cos\left(\frac{2n-1}{2}\pi\right) y dy = 0 \\ &\therefore F_n(t) = \int_{-1}^{1} F(y,t) \cos\left(\frac{2n-1}{2}\pi\right) y dy \\ F_n(t) = &\int_{-1}^{1} \left[\left(X_3 + \gamma_2 e^{-at}\right) \frac{\cosh m_1 y}{\cosh m_1}\right] \cos\left(\frac{2n-1}{2}\pi\right) y dy \\ = &\frac{2\left[\gamma_3 + \gamma_2 e^{-at}\right]}{\cosh m_1} \int_0^1 \cosh\left(m_1 y\right) \cos\left(\frac{2n-1}{2}\pi\right) y dy \end{aligned} \tag{35}$$

$$\begin{aligned} &F_n(t) = \gamma_1 \gamma_3 + \gamma_2 \gamma_1 e^{-at} \\ &\textit{Where} \quad \gamma_1 = \frac{(-1)^{n-1}(2n-1)\pi}{m_1^2 + \left(\frac{2n-1}{2}\pi\right)^2} \end{aligned} \tag{36}$$

From Eq. 34

$$\sum_{n=1}^{\infty}\left[P_r\frac{d}{dt}T_n^*(t)+\left(H_s+\left(\frac{2n-1}{2}\pi\right)^2\right)T_n^*(t)\right]\cos\left(\frac{2n-1}{2}\pi\right)=-\sum_{n=1}^{\infty}F_n(t)\cos\left(\frac{2n-1}{2}\pi\right)y \tag{37}$$

By orthogonality, we can get

$$\frac{dT_n^*(t)}{dt}+\frac{\left(H_s+\left(\frac{2n-1}{2}\pi\right)^2\right)}{P_r}T_n^*(t)=-\frac{F_n(t)}{P_r} \tag{38}$$

$$\frac{dT_n^*(t)}{dt}+\propto T_n^*(t)=\frac{-F_n(t)}{P_r} \tag{39}$$

where $\propto=\frac{H_s+\left(\frac{2n-1}{2}\pi\right)^2}{P_r}$, Then

$$T_n^*(t)=e^{-\propto t}\int\frac{-F_n(t)}{P_r}e^{\alpha t}dt+l_1e^{-\propto t} \tag{40}$$

at $t=0\quad T_n^*(t)=0$ then $\quad l_1=\frac{\gamma_1}{P_r}\left[\frac{\gamma_3}{\alpha}+\frac{\gamma_2}{(\propto -a)}\right]$

$$T_n(t)=\frac{\gamma_1}{P_r}\left[-\frac{\gamma_3}{\alpha}\left(1-e^{-\propto -t}\right)+\frac{\gamma_2}{(\propto -a)}\left(e^{-\propto t}-e^{-at}\right)\right] \tag{41}$$

$$\therefore T(t,y)=\left[\left(1-e^{-at}\right)\frac{\cosh m_1y}{\cosh m_1}\right]+\sum_{n=1}^{\infty}\frac{\gamma_1}{P_r}[-\frac{\gamma_3}{\alpha}\left(1-e^{-\alpha t}\right)+\frac{\gamma_2}{(\propto -a)}\left(e^{-\alpha t}-e^{-at}\right)\Big]\cos\left(\frac{2n-1}{2}\pi\right)y \tag{42}$$

Substituting Eq. 42 in 10 to get

$$\frac{\partial^2C(y,t)}{\partial y^2}-S_c\frac{\partial C(y,t)}{\partial t}-C_rS_cC(y,t)=-T_d\frac{\partial^2T(y,t)}{\partial y^2}$$
$$\text{at}\quad t=0\quad C=0\quad \text{For } y\in(-1,1)$$
$$\text{at}\quad t>0\quad C=\left(1-e^{-at}\right)\text{ For } y=\pm1 \tag{43}$$

To solve Eq. 43 by separation of variables method we first transform the non-homogenous boundary conditions to homogenous one. Let $C(y,t)=\left(1-e^{-at}\right)\frac{\cosh(m_2y)}{\cosh(m_1)}+C^*(y,t)$ For $t=0\quad C=0\quad \therefore C^*=0, t>0$ $C=\left(1-e^{-at}\right)$ at $y=\pm1\therefore C^*=0$

$$\therefore\frac{\partial^2C^*(y,t)}{\partial y^2}-S_c\frac{\partial C^*(y,t)}{\partial t}-C_rS_cC^*(y,t)=F_c(y,t) \tag{44}$$

$$F_c(y,t)=\left(\gamma_4+\gamma_5e^{-at}\right)\frac{\cosh\left(m_2y\right)}{\cosh\left(m_2\right)}-T_d(m_1)^2\left(1-e^{-at}\right)\frac{\cosh\left(m_1y\right)}{\cosh\left(m_1\right)}+T_d\sum_{n=1}^{\infty}\left(\frac{2n-1}{2}\pi\right)^2T_n(t)\cdot\cos\left(\frac{2n-1}{2}\pi\right)y \tag{45}$$

which can be written as

$$F_c(y,t)=\sum_{n=1}^{\infty}F_{nc}(t)\cdot\cos\left(\frac{2n-1}{2}\pi\right)y$$

By orthogonality

$$\therefore F_{nc}(t)=\int_{-1}^{1}F(y,t)\cos\left(\frac{2n-1}{2}\pi\right)ydy$$
$$F_{nc}(t)=\left(\gamma_4+\gamma_5e^{-at}\right)\gamma_6-\gamma_7\gamma_8\left(1-e^{-at}\right)+\gamma_9T_{nT}(t)$$
$$\gamma_4=\left(C_rS_c-m_2^2\right),\quad \gamma_5=\left[m_2^2+S_ca^2-C_rS_c\right]$$
$$\gamma_6=\frac{(-1)^{n-1}(2n-1)\pi}{m_2^2+\left(\frac{2n-1}{2}\pi\right)^2}\quad,\gamma_7=\gamma_1=\frac{(-1)^{n-1}(2n-1)\pi}{m_1^2+\left(\frac{2n-1}{2}\pi\right)^2}$$
$$\gamma_8=\left(-T_dm_1^2\right),\gamma_9=\left[\left(\frac{2n-1}{2}\pi\right)^2T_d\right]$$
$$\therefore\frac{\partial^2C^*(y,t)}{\partial y^2}-S_c\frac{\partial C^*(y,t)}{\partial t}-C_rS_c$$
$$C^*(y,t)=\sum_{n=1}^{\infty}F_{nc}(t)\cdot\cos\left(\frac{2n-1}{2}\pi\right)y \tag{46}$$

$$C^*(y,t)=\sum_{n=1}^{\infty}T_{nc}(t)\cdot\cos\left(\frac{2n-1}{2}\pi\right)y \tag{47}$$

By orthogonality, we can get

$$\frac{dT_{nc}(t)}{dt}+\frac{\left(C_rS_c+\left(\frac{2n-1}{2}\pi\right)^2\right)}{S_c}T_{nc}(t)=-\frac{F_{nc}(t)}{S_c} \tag{48}$$

$$T_{nc}(t)=\frac{-1}{S_c}\frac{\beta_4}{\alpha_1}\left(1-e^{-\alpha_1t}\right)-\frac{1}{S_c}\frac{\beta_5}{(\alpha_1-a)}\left(e^{-at}-e^{-\alpha_1t}\right)-\frac{\beta_6}{S_c(\alpha_1-\alpha)}\left(e^{-\alpha t}-e^{-\alpha_1t}\right) \tag{49}$$

where $\beta_1 = \left[\frac{\gamma_1}{P_r}\right]$, $\beta_2 = \left[\frac{\gamma_3}{\alpha}\right]$, $\beta_3 = \left[\frac{\gamma_2}{\alpha - a}\right]$, $\beta_4 = \gamma_4\gamma_6 - \gamma_7\gamma_8 + \beta_1\beta_2\gamma_9$, $\beta_5 = \gamma_5\gamma_6 + \gamma_7\gamma_8 - \beta_1\beta_3\beta_9$, $\beta_6 = \beta_1\beta_3\gamma_9 - \beta_1\beta_2\gamma_9$, $\alpha_1 = \frac{C_r S_c + \left(\frac{2n-1}{2}\pi\right)^2}{S_c}$

$$\therefore C(y,t) = \left[\left(1 - e^{-at}\right)\frac{\cosh m_2 y}{\cosh m_2}\right] + \sum_{n=1}^{\infty} T_{nc}(t) \cdot \cos\left(\frac{2n-1}{2}\pi\right)y \tag{50}$$

Solve Eq. 8 for u in to get

$$u = \tau\frac{\partial v}{\partial t} + v \tag{51}$$

Substitute Eq. 51 into Eq. 8 to get

$$\tau\frac{\partial^2 v}{\partial t^2} + \frac{\partial v}{\partial t} = \frac{dp}{dx} + G_r T + G_m C + \left(1 - V_e\frac{\partial}{\partial t}\right)\left(\tau\frac{\partial^3 v}{\partial t \partial y^2} + \frac{\partial^2 v}{\partial y^2}\right) - L\frac{\partial v}{\partial t} - \frac{1}{M}\left(\tau\frac{\partial v}{\partial t} + v\right) \tag{52}$$

$$\tau V_e\frac{\partial^4 v}{\partial t^2 \partial y^2} + V_e\frac{\partial^3 v}{\partial t \partial y^2} - \tau\frac{\partial^3 v}{\partial t \partial y^2} - \frac{\partial^2 v}{\partial y^2} + \left(1 + \frac{\tau}{M} + L\right)\frac{\partial v}{\partial t} + \frac{v}{M} + \tau\frac{\partial^2 v}{\partial t^2} = G_r T + G_m T - \frac{dp}{dx} \tag{53}$$

by substituting $v(y,t) = \sum_{n=1}^{\infty} T_{nv}(t)\cos\left(\frac{2n-1}{2}\pi\right)y$

$$\sum_{n=1}^{\infty}\left\{a_2 T''_{nv}(t) + b_2 T'_{nv}(t) + l_2 T_{nv}(t)\right\} \cdot \cos\left(\frac{2n-1}{2}\pi\right)y = \left(1 - e^{-at}\right)\left(G_r\frac{\cosh m_1 y}{\cosh m_1} + G_m\frac{\cosh m_2 y}{\cosh m_2}\right) + \sum_{n=1}^{\infty}\left(G_r T_{nT}(t) + G_m T_{nc}(t)\right)\cos\left(\frac{2n-1}{2}\pi\right)y - \frac{dP}{dx}$$

Where

$$a_2 = \tau\left(1 - V_e\left(\frac{2n-1}{2}\pi\right)^2\right), \frac{dP}{dx} = P(t),$$

$$b_2 = \left(1 + L + \frac{\tau}{M}\right) + (\tau - V_e)\cdot\left(\frac{2n-1}{2}\pi\right)^2$$

$$l_2 = \frac{1}{M} + \left(\frac{2n-1}{2}\pi\right)^2, T_{nT}(t) = \beta_1\beta_2 + (\beta_1\beta_3 - \beta_1\beta_2)e^{-\alpha t} - \beta_1\beta_3 e^{-at}$$

$$T_{nc}(t) = -\frac{\beta_4}{\propto S_c} - \frac{\beta_6}{(\alpha_1 - \propto)S_c}e^{-\propto t} - \frac{\beta_5}{(\alpha_1 - \propto)S_c}e^{-at} + \left(\frac{\beta_5}{S_c(\alpha_1 - a)} + \frac{\beta_6}{S_c(\alpha_1 - \propto)}\right)e^{-\alpha_1 t} \tag{54}$$

From Eq. 54 by using orthogonality

$$\int_{-1}^{1}\cos\left(\frac{2n-1}{2}\pi\right)y\cos\left(\frac{2m-1}{2}\pi\right)y dy = \begin{cases} 0 & m \neq n \\ 1 & m = n \end{cases}$$

$$\int_{-1}^{1}\cos\left(\frac{2m-1}{2}\pi\right)y\frac{\cosh m_1 y}{\cosh m_1}dy = \frac{(-1)^n(2n-1)\pi}{m_1^2 + \left(\frac{2n-1}{2}\pi\right)^2} = \gamma_7$$

$$\int_{-1}^{1}\cos\left(\frac{2m-1}{2}\pi\right)y\frac{\cosh m_2 y}{\cosh m_2}ydy = \frac{(-1)^n(2n-1)\pi}{m_2^2 + \left(\frac{2n-1}{2}\pi\right)^2} = \gamma_8$$

$$\int_{-1}^{1}P(t)\cos\left(\frac{2m-1}{2}\pi\right)ydy = 2P(t)\frac{(-1)^{n-1}}{\left(\frac{2n-1}{2}\pi\right)} = P(t).\gamma_{15}, \quad \gamma_{15} = \frac{2(-1)^{n-1}}{\left(\frac{2n-1}{2}\pi\right)}$$

$$a_2 T''_{nv}(t) + b_2 T'_{nv}(t) + l_2 T_{nv}(t) = \gamma_{11} + \gamma_{12}e^{-at} + \gamma_{13}e^{-\alpha t} + \gamma_{14}e^{-\alpha_1 t} - P(t)\gamma_{15}$$

Where

$$\gamma_{11} = \left[(\gamma_7 + \beta_1\beta_2)G_r + \left(\gamma_8 - \frac{\beta_4}{\alpha S_c}\right)G_m\right]$$

$$\gamma_{12} - \left[(\gamma_7 - \beta_1\beta_3)G_r + G_m\left(\gamma_8 - \frac{\beta_5}{(\alpha_1 - a)S_c}\right)\right]e^{-at}$$

$$\gamma_{13} = \left[G_r(\beta_1\beta_3 - \beta_1\beta_2) - G_m\left(\frac{\beta_6}{(\alpha_1 - \alpha)S_c}\right)\right]e^{-\alpha t}$$

$$\gamma_{14} = \left[\frac{\beta_5}{S_c(\alpha_1 - \alpha)} + \frac{\beta_6}{S_c(\alpha_1 - \alpha)}\right]G_m e^{-\alpha_1 t} \tag{55}$$

Consider the homogenous one

$$\mathrm{a_2\ T''_{nv}(t) + b_2\ T'_{nv}(t) + C_2\ T_{nv}(t) = 0} \tag{56}$$

The auxiliary equation and its roots are

$$a_2 m^2 + b_2 m + l_2 = 0, \quad m_1 = \frac{-b_2 + \sqrt{b_2^2 - 4a_2 l_2}}{2a_2}, \quad m_2 = \frac{-b_2 - \sqrt{b_2^2 - 4a_2 l_2}}{2a_2} \tag{57}$$

$$\therefore T_{nv_h}(t) = l_1 e^{m_1 t} + l_2 e^{m_2 t} \tag{58}$$

For non-homogenous one, the particular solution is

$$T_{nv_p}(t) = \frac{1}{a_2 D^2 + b_2 D + l_2}\left[\gamma_{11} + \gamma_{12}e^{-at} + \gamma_{13}e^{-\alpha t} + \gamma_{14}e^{-\alpha_1 t} - \gamma_{15}P(t)\right] \tag{59}$$

Case 1: $P(t) = a_0 e^{-a_1 t}$ a_0, a_1 are constants. The exponential pressure variation arises because of the no-slip boundary condition, which states that the fluid sticks to the plates and has zero velocity at the plates' surface. As a result, fluid particles near the plates experience a higher drag force than those far away from the plates. This difference in drag force creates a pressure gradient that drives the fluid flow. The particular solution is

$$T_{nv}(t) = \gamma_{16} + \gamma_{17} e^{-at} + \gamma_{18} e^{-\propto t} + \gamma_{19} e^{-\alpha_1 t} - \gamma_{20} e^{-a_1 t} \tag{60}$$

The general solution is

$$\begin{aligned} \mathrm{T_{nv}} =& \mathrm{C_1 e^{m_1 t}} + \mathrm{C_2 e^{m_2 t}} + \gamma_{16} + \gamma_{17} \mathrm{e^{-at}} \\ &+ \gamma_{18} \mathrm{e^{-\alpha t}} + \gamma_{19} \mathrm{e^{-\alpha_1 t}} - \gamma_{20} \mathrm{e^{-a_1 t}} \end{aligned} \tag{61}$$

where

$$\begin{aligned} &\gamma_{16} = \frac{\gamma_{11}}{l_2}, \quad \gamma_{17} = \frac{\gamma_{12}}{(a_2 a^2 - b_2 a + l_2)}, \gamma_{18} = \frac{\gamma_{13}}{(a_2 \alpha^2 - b_2 \alpha + l_2)}, \\ &\gamma_{19} = \frac{\gamma_{14}}{(a_2 \alpha_1^2 - b_2 \alpha_1^2 + l_2)}, \gamma_{20} = \frac{\gamma_{15} a_0}{(a_2 a_1^2 - b_2 a_1 + l_2)} \\ &\because \text{ at } t = 0 \quad T_{nv} = 0, \therefore 0 = l_1 + l_2 + \gamma_{16} + \gamma_{17} + \gamma_{18} + \gamma_{19} - \gamma_{20} \\ &\because \frac{a I_{nv}}{dt} = 0 \therefore 0 = m_1 l_1 + m_2 l_2 - a\gamma_{17} - \propto \gamma_{18} - \alpha_1 \gamma_{19} + a_1 \gamma_{20} \\ &\therefore l_1 = \frac{1}{(m_2 - m_1)} (-m_2 \gamma_{16} - (m_2 + a)\gamma_{17} - (m_2 + \propto)\gamma_{18} - (m_2 + \propto_1)\gamma_{19} + (m_2 - a_1)\gamma_{20}) \\ &\therefore l_2 = \frac{1}{(m_2 - m_1)} (m_1 \gamma_{16} + (m_1 + a)\gamma_{17} + (m_1 + \propto)\gamma_{18} + (m_1 + \alpha_1)\gamma_{19} - (m_1 - a_1)\gamma_{20}) \\ &v(y.t) = \sum_{n=1}^{\infty} T_{nv}(t) \cos\left(\frac{2n-1}{2}\pi\right) y \end{aligned} \tag{62}$$

$$\begin{aligned} T_{nu}(t) =& \tau \frac{dT_{nv}}{dt} + T_{nv} = l_1(1 + \tau m_1) e^{m_1 t} \\ &+ l_2(1 + \tau m_2) e^{m_2 t} + \gamma_{16} + (1 - \tau a)\gamma_{17} e^{-at} \\ &+ (1 - \tau \propto)\gamma_{18} e^{-\propto t} + (1 - \tau \propto_1)\gamma_{19} e^{-\alpha_1 t} \\ &- (1 - a_1 \tau)\gamma_{20} e^{-a_1 t} \end{aligned} \tag{63}$$

$$u(y,t) = \sum_{n=1}^{\infty} T_{nu}(t) \cos\left(\frac{2n-1}{2}\pi\right) y \tag{64}$$

Case 2: $P(t) = a_3 + a_4 t$, a_3, a_4 are constants. This case describes a uniform pressure gradient along the flow direction. The linear pressure variation arises when the fluid flow is in the fully developed region, i.e., when the velocity distribution has evolved completely and is maintained constant along the flow direction. In this case, the pressure drop proportionates to the distance between the plates, and the pressure variation is linear.

$$\begin{aligned} &\frac{1}{(a_2 D^2 + b_2 D + l_2)} \gamma_{15} P(t) = \frac{1}{a_2 (D - m_1)(D - m_2)} \gamma_{15} P(t) \\ &= \frac{1}{a_2 (m_1 - m_2)} \left(\frac{1}{D - m_1} - \frac{1}{D - m_2} \right) \gamma_{15} P(t) \\ &= \frac{1}{a_2 (m_1 - m_2)} \left[\frac{-1}{m_1} \left(1 - \frac{D}{m_1}\right)^{-1} + \right. \\ &\left. \frac{1}{m_2} (1 - D/m_2)^{-1} \right] P(t) \gamma_{15} \end{aligned} \tag{65}$$

$$\begin{aligned} \frac{1}{(a_2 D^2 + b_2 D + l_2)} \gamma_{15} P(t) =& \frac{1}{a_2} \left[\left(\frac{a_3}{m_1 m_2} + \frac{a_4 (m_1 + m_2)}{(m_1 m_2)^2} \right) \right. \\ &\left. + \frac{a_4}{m_1 m_2} t \right] \gamma_{15} = [a_5 + a_6 t] \gamma_{15} \end{aligned} \tag{66}$$

where

$$\begin{aligned} a_5 =& \left[\frac{a_3}{m_1 m_2 a_2} + \frac{a_4 (m_1 + m_2)}{(m_1 m_2) 2 a_2} \right] * \frac{1}{a_2}, \\ a_6 =& \frac{a_4}{m_1 m_2 a_2} * \frac{1}{a_2} T_{nv}(t) = l_1 e^{m_1 t} + l_2 e^{m_2 t} + \gamma_{16} \\ &+ \gamma_{17} e^{-at} + \gamma_{18} e^{-\propto t} + \gamma_{19} e^{-\alpha_1 t} + (a_5 + a_6 t)\gamma_{15} \end{aligned} \tag{67}$$

By applying the boundary conditions $at \quad t = 0 \quad T = 0$, $\frac{dT}{dt} = 0$, *weget*

$$\begin{aligned} l_1 =& \frac{1}{(m_2 - m_1)} [-m_2 \gamma_{16} - (m_2 + a)\gamma_{17} - (m_2 + \propto)\gamma_{18} \\ &- (m_2 + \propto_1)\gamma_{19} - a_5 m_2 \gamma_{15} + a_6 \gamma_{15}] \\ l_2 =& \frac{1}{(m_2 - m_1)} [+m_1 \gamma_{16} + (m_1 + a)\gamma_{17} + (m_1 + \propto)\gamma_{18} \\ &+ (m_1 + \alpha_1)\gamma_{19} + a_5 m_2 \gamma_{15} - a_6 \gamma_{15}] \\ T_{nv}(t) =& l_1 e^{m_1 t} + l_2 e^{m_2 t} + \gamma_{16} + \gamma_{17} e^{-at} + \gamma_{18} e^{-\alpha t} \\ &+ \gamma_{19} e^{-\alpha_1 t} + (a_5 + a_6 t)\gamma_{15} \end{aligned} \tag{68}$$

$$v(y,t) = \sum_{n=1}^{\infty} T_{nv}(t) \cos\left(\frac{2n-1}{2}\pi\right) y \tag{69}$$

$$\begin{aligned} T_{nu}(t) =& \tau \frac{dT_{nv}}{dt} + T_{nv} = l_1(\tau m_1 + 1)e^{m_1 t} \\ &+ l_2(\tau m_2 + 1)e^{m_2 t} + \gamma_{16} + (1 - \tau a)\gamma_{17} e^{-at} \\ &+ (1 - \tau \propto)\gamma_{18} e^{-\alpha t} + (1 - \tau \propto_1)\gamma_{19} e^{-\alpha_1 t} \\ &+ (a_5 + a_6 t + \tau a_6)\gamma_{15} \end{aligned} \tag{70}$$

$$u(y,t) = \sum_{n=1}^{\infty} T_{nu}(t) \cos\left(\frac{2n-1}{2}\pi\right) y \tag{71}$$

3 Results

The analytical solutions for partial differential equations have been carried out, and results are displayed for temperature, concentration, and velocity profiles for two different cases of pressure distribution. The calculation of flow rate for a constant pressure gradient is easier than for an exponential pressure gradient. As opposed to that, the exponential pressure gradient is more realistic than the constant pressure gradient. The exponential pressure gradient can lead to more stable flow conditions than the constant pressure gradient.

The physical quantities for engineering applications, local Nusselt number $Nu = -(\delta T/\delta y)_{y=0}$, and local Sherwood number $Sh = -(\delta C/\delta y)_{y=0}$ are defined as [26]. The current results are compared with the previously published available results for different cases, which obtained numerically by Abass et al. [26], in order to investigate the validity of the current results and procedures. The values are shown in Table 1. Nusselt and Sherwood numbers have been compared for various parameters. The current results showed good agreement.

The analytical results for temperature, concentration, fluid velocity, and dust velocity showed good agreement with Madhura and Kalpana [25] as shown in Tables 2 and 3

Table 1 Comparison of Nusselt number and local Sherwood number

γ	G_m	S_c	G_r	P_r	*Nusselt number*		*Sherwood number*	
					Present	**Abbas et al. 2023**	**Present**	**Abbas et al. 2023**
0.8	5.0	0.4	8.0	0.4	0.688	0.686	1.452	1.467
0.8	5.0	0.4	8.0	0.4	0.276	0.278	1.812	1.998
0.8	5.0	0.4	8.0	0.4	0.388	0.385	1.511	1.510
1.6	3.0	0.4	5.0	0.6	0.398	0.396	1.983	1.981
1.6	3.0	0.4	5.0	0.6	0.249	0.247	2.911	2.864
1.6	3.0	0.4	5.0	0.6	0.512	0.513	2.879	2.821

Table 2 Comparisons of temperature and concentration

	Temperature			**Concentration**		
Y	**Present**	**Madhura and Kalpana 2013**	**% error**	**Present**	**Madhura and Kalpana 2013**	**% error**
0.2	0.124	0.125	0.8	0.162	0.164	1.2
0.5	0.144	0.146	1.4	0.168	0.169	0.6
0.8	0.196	0.193	1.6	0.189	0.191	1

Table 3 Comparisons of fluid and dust velocities

	Fluid Velocity			**Dust Velocity**		
Y	**Present**	**Madhura and Kalpana 2013**	**% error**	**Present**	**Madhura and Kalpana 2013**	**% error**
0.2	1.53	1.51	1.3	0.52	0.51	2
0.5	1.94	1,91	1.6	1.21	1.19	1.7
0.8	1.51	1.52	0.7	1.22	1.21	0.8

4 Discussions

Figures 2 and 3 show the influence of Prandtl number P_r and the heat source or heat sink coefficient H_s on temperature. It has been noted that the more temperature increase, the more Pr and H_s decrease. Figures 4 and 5 confirm that the concentration of the fluid increases when the thermal diffusion parameter Td increases and the Schmidt number Sc decreases, respectively. Figure 6 confirms that the concentration of the fluid increases when the heat source or heat sink coefficient H_s decreases. Figure 7 confirms that the concentration of the fluid increases when the Prandtl number Pr increases. Figures 8, 9, 10, and 11 represent the fluid and dust velocities profiles. These figures confirm that fluid and dust velocities increase as Td increases. Figures 12, 13, 14, and 15 show that the fluid and dust velocities increase when Cr decreases. Figures 16 and 17 represent the influence of time on the temperature and the concentration,

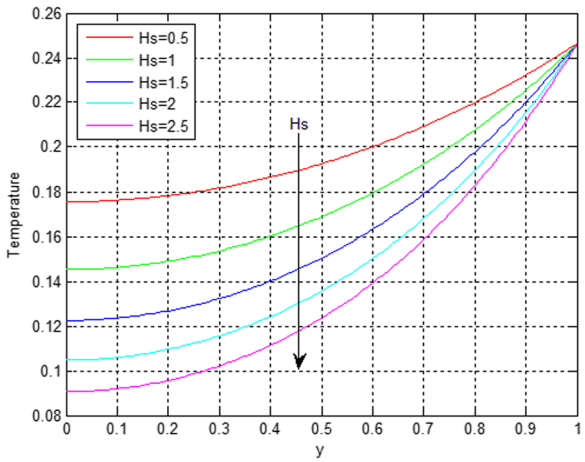

Fig. 2 Variation of temperature with H_s

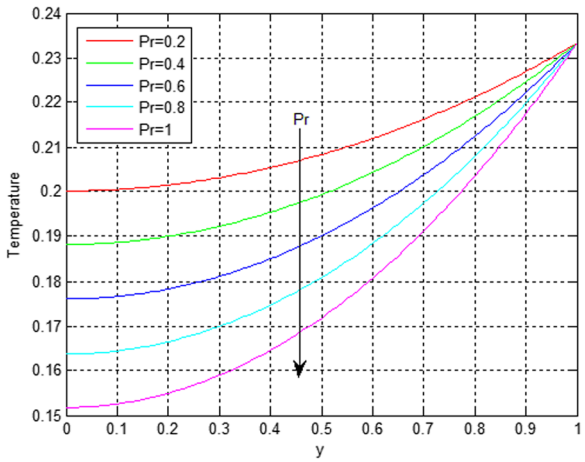

Fig. 3 Variation of temperature with P_r

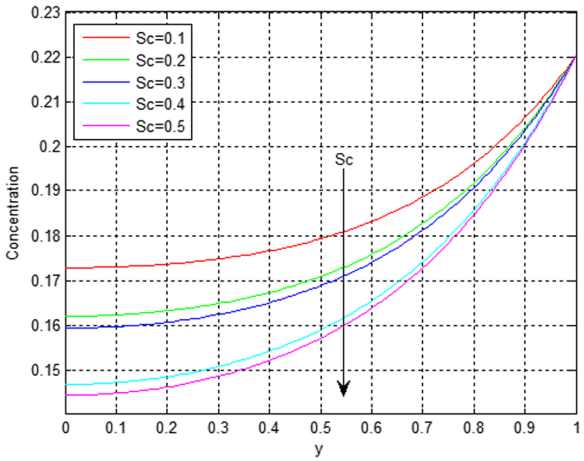

Fig. 4 Variation of concentration with S_c

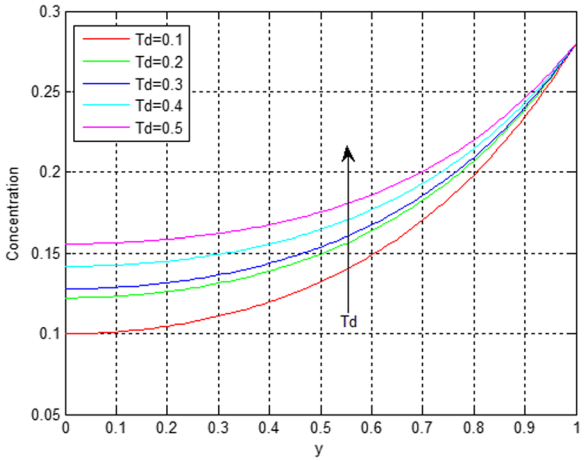

Fig. 5 Variation of concentration with T_d

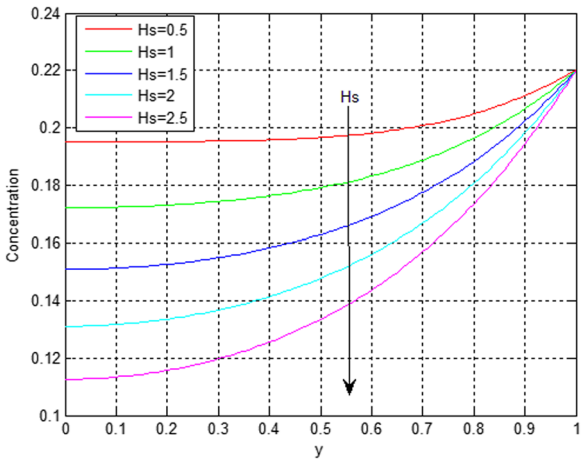

Fig. 6 Variation of concentration with H_s

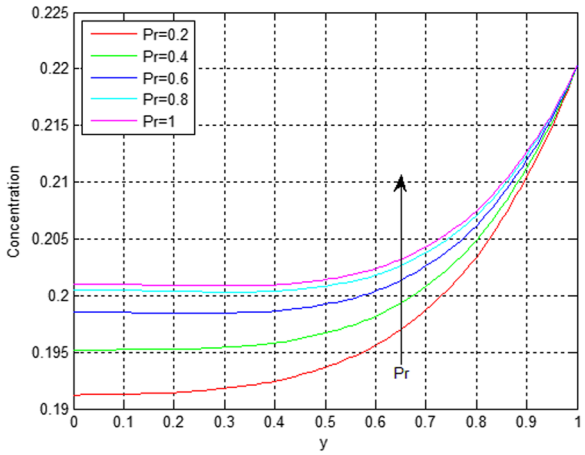

Fig. 7 Variation of concentration with P_r

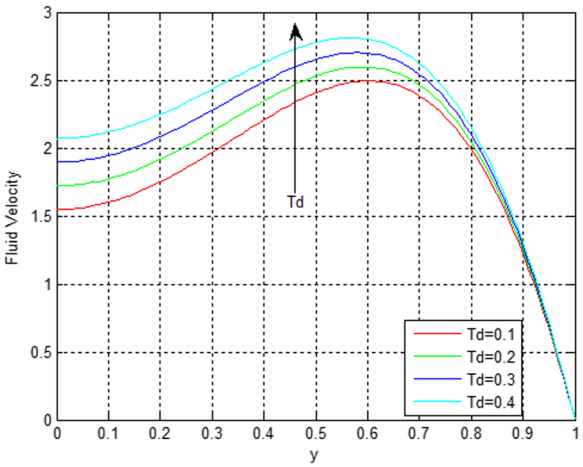

Fig. 10 Variation of fluid velocity with C_r-case 1

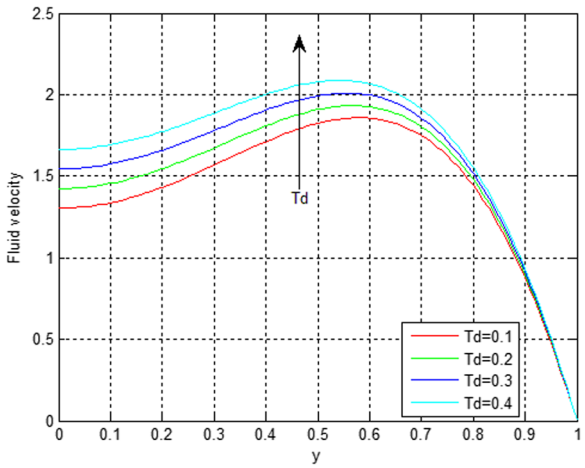

Fig. 8 Variation of fluid velocity with T_d-case 1

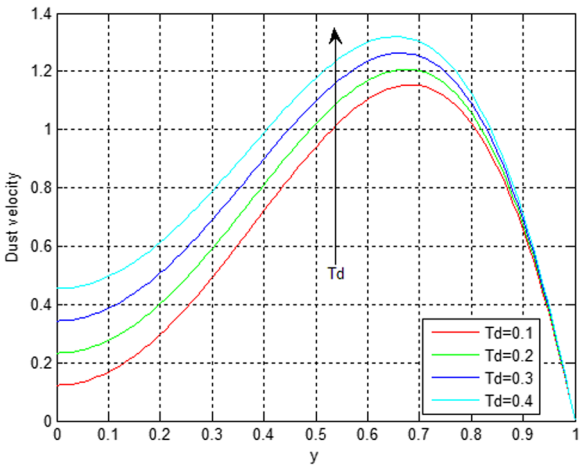

Fig. 11 Variation of dust velocity with C_r-case 1

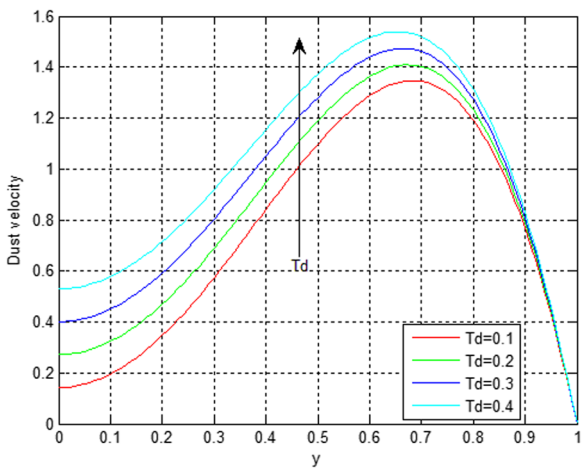

Fig. 9 Variation of dust velocity with T_d-case 1

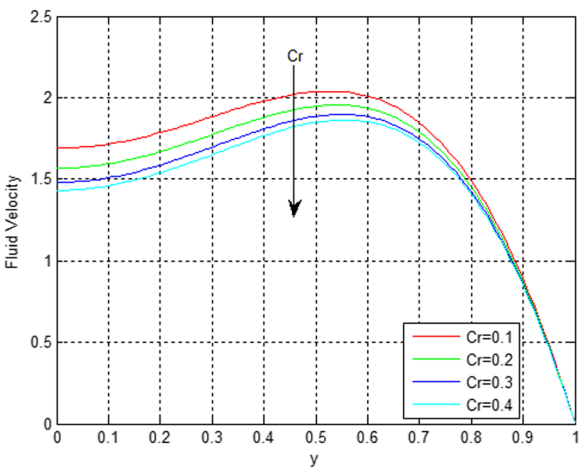

Fig. 12 Variation of fluid velocity with T_d-case 2

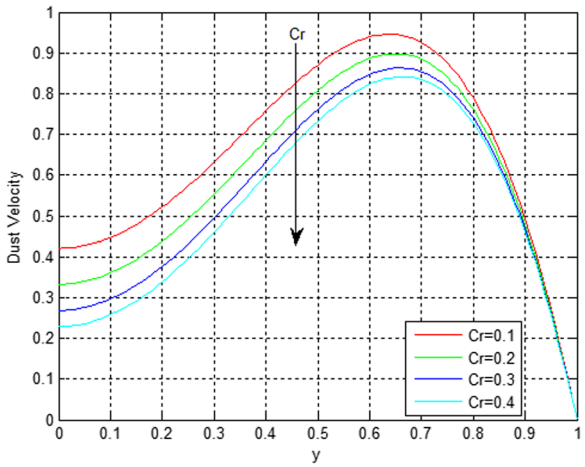

Fig. 13 Variation of dust velocity with T_d-case 2

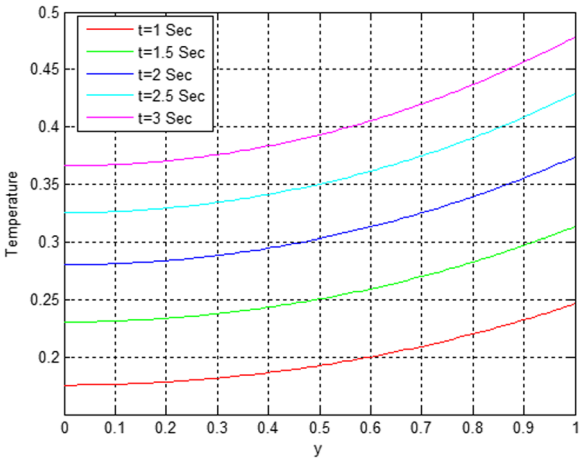

Fig. 16 Variation of temperature with time

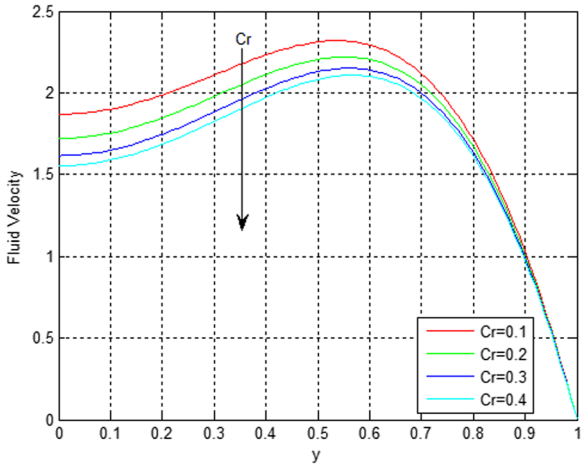

Fig. 14 Variation of fluid velocity with C_r-case 2

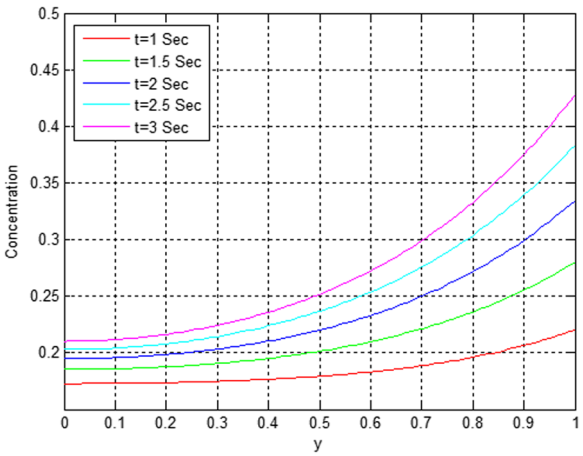

Fig. 17 Variation of concentration with time

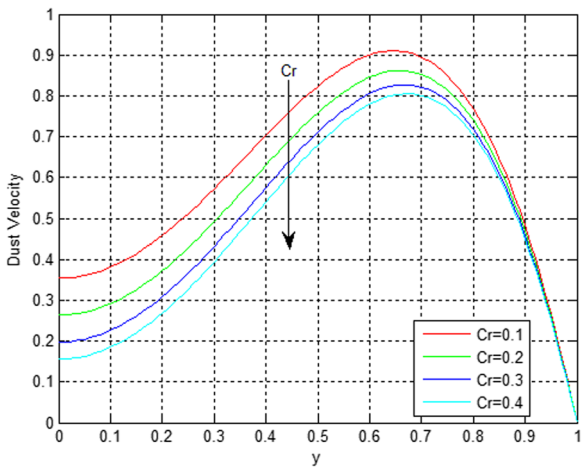

Fig. 15 Variation of dust velocity with C_r-case 2

respectively. The temperature and concentration increase as time increases. The graphs are based on the following values:

$$c_{\mathrm{r}} = 0.4, a = 0.2, H_{\mathrm{s}} = 0.2, t = 1, P_{\mathrm{r}} = 0.4,$$
$$S_{\mathrm{c}} = 0.6, M = 10, l = 0.1, D = 1, V_{\mathrm{e}} = 0.3,$$
$$\tau = 0.9, G_{\mathrm{m}} = 5, G_{\mathrm{r}} = 10n = 2, a_0 = 2.5,$$
$$a_1 = 0.3, a_3 = 2.5, a_4 = 0.2 \text{ and } m_2 = 1.5$$

5 Conclusion

The exact expressions for temperature, concentration, and velocity profiles for fluid and dusty particles are derived analytically. Results are displayed graphically for the various values of parameters. The key discovery may be summed up as follows:

- The temperature is inversely proportional to both the Prandtl number Pr and the heat source and sink parameter H_s.
- The concentration of the fluid is inversely proportional to the thermal diffusion parameter Td and the heat source or heat sink parameter H_s.
- The fluid concentration is proportional to Schmidt's number Sc and Prandtl's number Pr
- Fluid and dust particle velocities increase as *Td* increases.
- Fluid and dust particle velocities increase as Cr decreases.
- If the dust particles are very fine, i.e., the mass of the dust particles is very small, and as $\tau - > 0$ the velocities of the fluid and dust particles will be the same.
- The temperature and concentration increase with time.

The proposed analytical method will be used to study more complex problems that include chemical, ion slip, and magnetohydrodynamic effects on dusty fluid flow with mass and heat transfer in a porous media.

Abbreviations

MHD	Magnetohydrodynamic
PDE	Partial differential equation
Pr	Prandtl number
Nu	Nusselt number
Sh	Local Sherwood number

Acknowledgements
Not applicable

Author contributions
MA, team leader, initiated the concept of the current paper and derived the governing equations. SA performed the analytical solution. OK performed a parametric study for different cases. ME and WA conducted the discussion of results and reviewed the manuscript. All authors have read and approved the manuscript.

Funding
Not applicable

Availability of data and materials
Not applicable

Declarations

Ethics approval and consent to participate
Not applicable

Consent for publication
Not applicable

Competing interests
The authors declare that they have no competing interests.

Author details
[1]Department of Engineering Math and Physics, Faculty of Engineering, Cairo University, Giza, Egypt. [2]Smart Engineering Systems Center (SESC), Nile University, Shaikh Zayed, Giza, Egypt. [3]Department of Engineering Math and Physics, Faculty of Engineering, Cairo University, Giza, Egypt. [4]Basic and Applied Science Department, College of Engineering and Technology, Arab Academy for Science, Technology, and Maritime Transport, Cairo, Egypt. [5]Department of Engineering Math and Physics, Faculty of Engineering, Cairo University, Giza, Egypt.

Received: 12 February 2023 Accepted: 1 August 2023
Published online: 29 August 2023

References

1. Pandya N, Quraishi MS (2018) Effect of variable permeability, concentration and viscous dissipation with chemical reaction and oscillating temperature on unsteady mhd walters-b viscoelastic dusty fluid past over inclined porous. Int J Sci Res Math Stat Sci 5(4):33
2. Ali F, Bilal M, Sheikh NA, Khan I, Nisar KS (2019) Two-phase fluctuating flow of dusty viscoelastic fluid between non-conducting rigid plates with heat transfer. IEEE Access 7:123299–123306. https://doi.org/10.1109/ACCESS.2019.2933529
3. Radhika M, Punith Gowda RJ, Naveenkumar R, Siddabasappa Prasannakumara BC (2021) Heat transfer in dusty fluid with suspended hybrid nanoparticles over a melting surface. Heat Transfer 50:2150–2167. https://doi.org/10.1002/htj.21972
4. Patre S, Kurre RK (2022) Thermodynamic and volumetric properties of hydroxamic acids in dimethylsulfoxide. Chem Thermodyn Therm Anal 7:100066
5. Bilal M, Khan S, Ali F, Arif M, Khan I, Nisar KS (2021) Couette flow of viscoelastic dusty fluid in a rotating frame along with the heat transfer. Sci Rep 11(1):506
6. Reddy B, Kesavaiah DC, Reddy GVR (2018) Effects of radiation and thermal diffusion on mhd heat flow of a dusty viscoelastic fluid between two moving parallel plates. J Eng Appl Sci 13(22):8863–8872
7. Govindarajan A, Vijayalakshmi R, Ramamurthy V (2018) Combined effects of heat and mass transfer to magneto hydrodynamics oscillatory dusty fluid flow in a porous channel. J Phys: Conf Ser. https://doi.org/10.1088/1742-6596/1000/1/012003
8. Suneetha K, Ibrahim SM, Vijaya Kumar P, Jyothsna K (2021) Linear thermal radiation effects on MHD viscoelastic fluid flow through porous moving plate with first order chemical reaction, variable temperatureand concentration. J Comput Appl Res Mech Eng 10(2):496-509. https://doi.org/10.22061/jcarme.2020.2599.1258
9. Dey D, Chutia B (2022) Modelling and analysis of dusty fluid flow past a vertical surface with exothermic and endothermic kind of chemical reactions. In: Mahanta P, Kalita P, Paul A, Banerjee A (eds) Advances in thermofluids and renewable energy. Springer, Singapore, pp 45–57
10. Prasanthi TBM (2020) Radiation and chemical reaction effects on mhd flow of dusty fluid over inclined porous plate embedded in porous medium. Solid State Technol 63(6):17800–17814
11. Ojha KL, Swain K, Dash P (2022) Viscoelastic hydromagnetic oscillatory flow in a channel in the presence of sinusoidal pressure gradient and linear motion of the plate. Heat Transf 51(1):1138–1149. https://doi.org/10.1002/htj.22345
12. Dash GC, Ojha KL (2018) Viscoelastic hydromagnetic flow between two porous parallel plates in the presence of sinusoidal pressure gradient. Alex Eng J 57(4):3463–3471. https://doi.org/10.1016/j.aej.2017.12.011
13. Jadav K (2018) Soret and dufuor effects on unsteady hydromagnetic dusty fluid flow past an exponentially accelerated plate with variable viscosity and thermal conductivity. Front Heat Mass Transfer 10(29):1–18. https://doi.org/10.5098/hmt.10.29[39]
14. Bilal M, Ramzan M (2019) Hall current effect on unsteady rotational flow of carbon nanotubes with dust particles and nonlinear thermal radiation in darcy-forchheimer porous media. J Therm Anal Calorim 138:3127–3137
15. Dawar A, Shah Z, Kumam P, Alzahrani AK, Khan W, Thounthong P (2019) Impact of volume fraction and hall effect on two-phase radiative dusty nanofluid flow over a stretching sheet. IEEE Access. https://doi.org/10.1109/ACCESS.2019.2937389
16. Singh N, Kumar S (2019) Hydromagnetic instability of density stratified rotating layer of Rivlin-Ericksen visco-elastic fluid in porous medium. Int J Math Trends Technol 65:200–217

17. Chitra M, Kavitha V (2017) Influence of slip condition on unsteady pulsatile flow through a porous medium in a circular pipe. Res J Sci Technol 9(3):441
18. Kumar S, Pundir R, Nadian PK (2020) Effect of dust particles on a rotating couple-stress ferromagnetic fluid heated from below. Int J Sci Eng Appl Sci
19. Sasikala R, Govindarajan AG, Gayathri R (2018) Unsteady stokes flow of dusty fluid between two parallel plates through porous medium in the presence of magnetic field. J Phys Conf Series 1000
20. Farhad A, Muhammad B, Madeha G, Ilyas K (2020) A report on fluctuating free convection flow of heat absorbing viscoelastic dusty fluid past in a horizontal channel with mhd effect. Sci Rep. 10(1):8523
21. Heshmat T, Elshabrawy M (2021) Analytical solution for nonlinear interaction of euler beam resting on a tensionless soil. Proc Int Struct Eng Constr 8(1):02–1026
22. Keane P, Jacob R, Trout N, Clarke S, Bruno F (2021) Thermal stability of a waste-based alkali-activated material for thermal energy storage. Chem Thermodyn Therm Anal 3–4:100014
23. Elshabrawy M, Abdeen MA, Beshir S (2021) Analytic and numeric analysis for deformation of non-prismatic beams resting on elastic foundations. Beni-Suef Univ J Basic Appl Sci 10:1–1
24. Al-Raeei M (2022) Bulk modulus for morse potential interaction with the distribution function based. Chem Thermodyn Therm Anal 6:100046
25. MadhuraK R, Kalpana G (2013) Thermal effect on unsteady flow of a dusty visco-elastic fluid between two parallel plates under different pressure gradients. Int J Eng Technol 2:88–99
26. Abbas W, Khaled O, Beshir S, Abdeen M, Elshabrawy M (2023) Analysis of chemical, ion slip, and thermal radiation effects on an unsteady magnetohydrodynamic dusty fluid flow with heat and mass transfer through a porous media between parallel plates. Bull Natl Res Centre 47(49):1

Publisher's Note